Available online at www.sciencedirect.com
ScienceDirect
Carbohydrate Polymers 69 (2007) 41–49
Carbohydrate Polymers
www.elsevier.com/locate/carbpol

Chitosan/organic rectorite nanocomposite films: Structure, characteristic and drug delivery behaviour

Xiaoying Wang [a], Yumin Du [a,*], Jiwen Luo [a], Baofeng Lin [a], John F. Kennedy [b]

[a] *Department of Environmental Science, College of Resource and Environmental Science, Wuhan University, Wuhan 430072, China*
[b] *Birmingham Carbohydrate and Protein Technology Group, Chembiotech Laboratories, University of Birmingham Research Park, Vincent Drive, Birmingham B15 2SQ, UK*

Received 29 August 2006; accepted 29 August 2006
Available online 13 November 2006

Abstract

Rectorite is a kind of layered silicate, with the structure and characteristic much like those of montmorillonite. It is a regularly interstratified clay mineral with alternate pairs of dioctahedral mica-like layers (nonexpansible) and dioctahedral montmorillonite-like layers (expansible) in a 1:1 ratio. Chitosan/organic rectorite (chitosan/OREC) nanocomposite films with different mass ratios of chitosan to organic rectorite and corresponding drug-loaded films were successfully obtained by a casting/solvent evaporation method. The structures of the films were evaluated by FTIR-ATR, XRD and SEM. A wide variety of material characteristics for the chitosan/OREC nanocomposite films were investigated, including the water resistance, mechanical property, optical transmittance, anti-ultraviolet capacity and bactericidal activity. The characteristics of the nanocomposite films were related to the amount and the interlayer distance of OREC in them. *In vitro* drug-controlled release studies showed a slower and more continuous release for the nanocomposite films in comparison with pure chitosan film, and the drug-delivery cumulative release was proportional to the amount and the interlayer distance of OREC. The chitosan/OREC nanocomposites films provide promising applications as antimicrobial agents, water-barrier compounds, anti-ultraviolet compounds, and drug-controlled release carriers in antimicrobial food packaging and drug-delivery system.

Keywords: Chitosan; Organic rectorite; Nanocomposite; Drug delivery

1. Introduction

Petroleum-based films dominate today's food packaging and other industrial applications such as in the wastewater treatment, cosmetics and biomedicine industries, because of their high strength, light-weight, low-cost, easy processing, etc. However, most synthetic polymers are not biodegradable. Environmental issues are becoming increasingly serious for the environment and to the consumer, so more research has been done to utilize biodegradable polymers (Petersen et al., 1999).

Chitosan is one of the most abundant natural aminopolysaccharides. It has been widely used in food production for clarification and deacidification of fruit juices (fining agent), for purification of water, for antioxidative maintenance in muscle foods, etc., (Shahidi, Arachchi, & Jeon, 1999) and in pharmaceutical areas, e.g. for drug-delivery systems (Vilivalam & Dodane, 1998) because it has good biocompatibility, biodegradability, film-forming property and antimicrobial activity (Ravi & Majeti, 2000). In order to widen its application, many attempts have been made to optimize its properties, such as by cross-linking (Lopez & Bodmeier, 1997; Wei, Hudson, & Mayer, 1992), blending (Perugini, Genta, Conti, Modena, & Pavanetto, 2003; Rujiravanit, Kruaykitanon, Jamieson, & Tokura, 2003; Wang, Du, & Fan, 2005) and formation into chitosan-based composites (Li, Du, Zhang, & Pang, 2003).

Rectorite is a kind of layered silicate; with the structure and characteristic much like those of montmorillonite. It is

* Corresponding author. Tel./fax: +86 27 68778501.
E-mail address: duyumin@whu.edu.cn (Y. Du).

0144-8617/$ - see front matter © 2006 Elsevier Ltd. All rights reserved.
doi:10.1016/j.carbpol.2006.08.025

a regularly interstratified clay mineral with alternate pairs of dioctahedral mica-like layer (nonexpansible) and dioctahedral montmorillonite-like layer (expansible) in a 1:1 ratio. The thickness of a single rectorite layer is about 2 nm and the width and length vary from a micron to several microns. The interlayer cations of montmorillonite-like layers can be exchanged easily by either organic or inorganic cations, and therefore rectorite has a water swelling property similar to that of montmorillonite, which makes it possible to prepare chitosan/rectorite nanocomposites by solution-mixing processing technique. In this study therefore, an attempt has been made to intercalate chitosan into the interlayers of the silicate, with a view to exhibiting this as an attractive way to develop new organic–inorganic hybrid materials provided with properties that are inherent to both types of components.

In other ways, it is interesting to note that the layered silicate is a kind of a potent detoxifier, which can adsorb dietary toxins, bacterial toxins associated with gastrointestinal disturbance, hydrogen ions in acidosis, and metabolic toxins such as steroidal metabolites associated with pregnancy (Dong & Feng, 2005). The layered silicate can also provide mucoadhesive capability to cross the gastrointestinal barrier (Phillips, Lemke, & Grant, 2002), the incorporation of the layered silicate in the formulation being able to enhance significantly the interactions between nanoparticles and cells (Dong & Feng, 2005). Therefore, with good biocompatibility properties, such have been used in cosmetics as aesthetic medicine (to clean and moisturise the skin and to combat compact lipodystrophies, acne, and cellulite) (Zhao, Wang, & Hu, 2004), packaging (Avella et al., 2005) and in pharmaceutical areas such as gastrointestinal protectors, laxatives, antidiarrhoeaics and also as drug carrier and suspending agent (Carretero, 2002; Iborra et al., 2006). However, there are scarcely any reports about antibacterial agents or drug carriers which are composed of polymer/layered silicate nanocomposites.

Pure rectorite is hydrophobic and the affinity between rectorite and polymer is not enough, so rectorite must be modified in order to increase the affinity between rectorite and polymer. Organic rectorite (OREC) is calcium rectorite modified by cetyltrimethyl ammonium bromide. The preparation and characterization of both organic rectorite (OREC) and chitosan/OREC nanocomposites powder with different chitosan-OREC mass ratios have previously been satisfactorily investigated (Wang et al., 2006). The results indicated good intercalation of the polymeric phase into clay interlayer galleries. The objective of this new study was to prepare chitosan/OREC nanocomposite films and to evaluate their water resistance, mechanical property, anti-ultraviolet capacity, optical transmittance, and bactericidal activity. These nanocomposite films were also successfully loaded with bovine serum albumin (BSA), as a kind of model drug and the drug-controlled delivery behavior of the films was studied.

2. Experimental

2.1. Materials

Chitosan (chitosan) from shrimp shells was purchased from Yuhuan Ocean Biochemical Co. (Taizhou, China). The degree of deacetylation was 92% (determined by elemental analysis) (Xu, McCarthy, & Gross, 1996) and its weight average molecular weight was 2.1×10^5 (determined by a GPC method) (Qin, Du, & Xiao, 2002).

Calcium rectorite (Ca^{2+}-REC, frequently simply termed rectorite) refined from clay minerals was provided by Hubei Mingliu Inc. Co. (Wuhan, China). Cetyltrimethyl ammonium bromide (CTAB) was supplied by Xinrui Science and Technology Inc. Co. (Wuhan, China). Bovine serum albumin (BSA, $Mv = 6.8 \times 10^4$), a biochemical reagent, was purchased from Sigma Chemical Co. (St. Louis, MO). Tripolyphosphate (TPP) and all other chemicals were of analytical grade.

2.2. Preparation of chitosan and chitosan/OREC nanocomposite films and the corresponding drug-loaded films

First, the organic rectorite (OREC) was prepared by cation exchange between Ca^{2+}-rectorite galleries and CTAB in an aqueous solution. Then chitosan/OREC nanocomposites with different ratios were successfully prepared via a solution-mixing processing technique, as described in a previous paper (Wang et al., 2006), the products being in powder form.

Chitosan and chitosan/OREC nanocomposite films and corresponding drug-loaded films were prepared by a casting/solvent evaporation technique in which chitosan and chitosan/OREC nanocomposite powder with different chitosan-OREC mass ratios (2:1, 6:1, 12:1, 20:1, 50:1) were dissolved in a 2% (w/v) aqueous acetic acid to give 2% (w/v) chitosan and chitosan/OREC nanocomposite solutions. The solutions were poured onto a Teflon plate after air bubbles had been removed. The films were dried at room temperature to a constant weight. The final films were respectively designated as CR1, CR2, CR3, CR4, and CR5, their Δd_L values (the interlayer distance) were 3.29, 3.7, 8.24, 3.34 and 3.12 nm, respectively. The interlayer distance points to the distance between a rectorite layer and another rectorite layer, and it represents the extent to which chitosan can have intercalated into the interlayers of rectorite. The value of the interlayer distance can be determined by XRD patterns from 0.7° to 10° and TEM micrographs, as given in a previous paper (Wang et al., 2006). The thickness of the dried films was determined as $30 \pm 5\mu m$ (measured by a Peacock digital thickness gauge model PDN12N, Peacock, Tokyo, Japan).

Preparation of corresponding drug-loaded chitosan and chitosan/OREC nanocomposite films was similarly performed. In addition, BSA (0.1 g) was dissolved in 25 ml of each of these six solutions. The solutions were thoroughly stirred and left overnight to get rid of air bubbles before

being cast on to clean Teflon plates in a dust-free atmosphere at room temperature. Subsequently, the dried films were immersed for 15 min in a 1% (w/v) TPP solution to crosslink. Then the films were washed with the distilled water, placed on a Teflon plate and dried at room temperature until reaching a constant weight (films chitosan B, CRB1, CRB2, CRB3, CRB4, and CRB5). The thicknesses of the films was kept constant by the same weight solution was poured onto the same size Teflon plate between $30 \pm 5\mu m$.

2.3. Characterizations of the films

Fourier transform infrared (FTIR) spectroscopy in combination with the attenuated total reflectance (ATR) technique was applied to this study, the FTIR-ATR spectra being recorded by a Nicolet FT-IR 5700 spectrophotometer (Nicolet, Madison, USA).

The X-ray diffraction (XRD) experiment was performed using a diffractometer type D/max-rA (Tokyo, Japan). The scanning rate was 4°/min and the scanning scope of 2θ was 5°–45° at room temperature.

The upper surface and fracture surface morphologies of the drug-loaded films were examined using a Hitachi XA-650 scanning electron microscope (SEM; Hitachi, Osaka, Japan). Samples were cryo-fractured from liquid nitrogen, and for morphological studies films of samples were mounted on metal grids, using double-sided adhesive tape, and coated with gold under vacuum.

2.4. Study on characteristics of the films

The water vapor permeability (WVP) of the films was measured according to an ASTM method (1993) in a constant relative humidity medium of 83% at 25 °C. In addition, the water uptake (Q%) of the films was assessed according to ISO62-1980(E), when a film was immersed in water at room temperature for 48 h.

The tensile strength (σ_b) and the elongation at break (ε_b) of the films were measured by a universal testing machine (CMT6503, Shenzhen SANS Test Machine Co. Ltd., Shenzhen, China) at a tensile speed of 50 mm/min according to ISO6239-1986(E). To obtain the mechanical properties of the films in the wet state, the films were soaked in water for 30 min at room temperature before testing.

Optical transmittance was performed by ultraviolet–visible spectrophotometry (Lambda 900, Perkin-Elmer, Boston, American) at 800 nm. Anti-ultraviolet properties of the films were detected by the same instruments under wavelengths of 297, 313, 350, 366, and 400 nm, and the ultraviolet screening factor was read directly from the ultraviolet–visible spectrophotometer.

2.5. Bactericidal assay

Gram-positive *Staphylococcus aureus* and Gram-negative *Escherichia coli* bacteria were provided by the China Center for Type Culture Collection (CCTCC at Wuhan University, China). The microorganism suspension was diluted by sterile distilled water to $\sim 10^6$ CFU/cell and then added into a set of six tubes with 25 ml aliquots of 0.9% w/v sterile saline. Chitosan film and the nanocomposites films which had been autoclaved were weighed into the tubes. Other tubes without samples served as the control. All tubes were agitated on an orbital shaker at 37 °C for 24 h. Portions (10 μl) were gradually diluted by 10-fold, and a 50-μl aliquot of the final dilution (i.e. the dilution which would give the numbers of colonies on one plate would be between 30 and 300) was plated uniformly using 'L-stick' – a tool which distributes the microorganism suspension uniformly onto the nutrient medium on nutrient medium (peptone 1%, beef extract 0.5%, NaCl 0.5%, agar 2%, pH 7.2). The plates were incubated at 37 °C for 24 h, after which the numbers of colonies on each plate were counted. The percent reductions in plate colonies were calculated by comparing the experimental plates with the controls. All the data were the means of at least three parallel experiments such that discrepancies among them were less than 5%.

2.6. In vitro drug-delivery study

The drug-loaded films were immersed in 50 ml aliquots of 0.1 M sodium phosphate buffer containing 0.85% sodium chloride, pH 7.4 (PBS), and incubated on a constant temperature shaking bed at 37 °C and 130 rpm. After specific intervals, 1 ml aliquot of samples were withdrawn and immediately replaced with the same amount of fresh medium. The BSA amounts in the samples withdrawn were quantified spectrophotometrically by a modified Coomassie Blue protein assay (Pierce Inc., New York, NY, USA) at 595 nm. The sample from the non-drug-loaded chitosan film was taken as the control. All the experiments were done in triplicate and mean values were reported.

3. Results and discussion

3.1. Structure and morphology characterization

The FTIR-ATR spectra (Fig. 1a) of the nanocomposite films and pure chitosan film were studied and compared, respectively, to examine the interactions between chitosan and OREC of the films. For all the films, the spectra of both sides (surface reflectance IR) have the same number of peaks, with similar positions and relative intensities. However, as compared to the spectra of the pure chitosan film, the frequency of vibration bands at 1595 cm^{-1} in the nanocomposite films, which corresponds to the deformation vibration of the protonated amine group, are shifted towards lower frequency values. This shift appears as a result of the electrostatic interaction between amine groups and the negatively charged sites in the clay structure, and is consistent with data in a previous report (Darder, Colilla, & Hitzky, 2003). In the FTIR-ATR spectra of all the

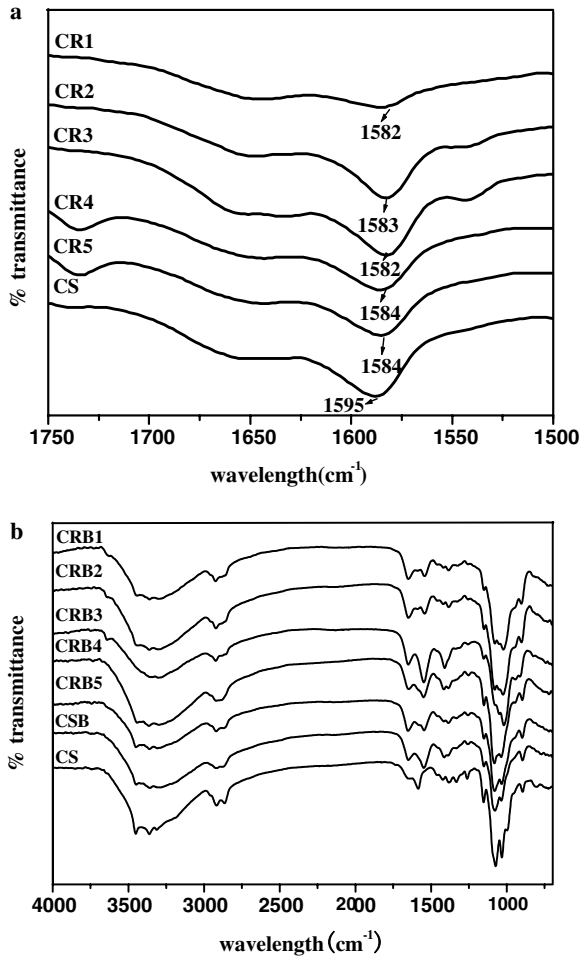

Fig. 1. (a) FTIR-ATR spectra of chitosan film and nanocompopsite films. (b) FTIR-ATR spectra of chitosan film, drug-loaded chitosan and CS/OREC nanocomposite films.

drug-loaded films (Fig. 1b), the broad band at 3300–3450 cm^{-1}, which is stretching vibrations of hydroxyl, amino and amide groups (Li et al., 2003), becomes broader and weaker or even disappears, which implies strong interactions between chitosan and OREC of the films and BSA.

In the XRD profiles of the films (Fig. 2), chitosan film is in a crystalline state because two main diffraction peaks ($2\theta = 15.4$ and 22.1) are observed. After being formed into the nanocomposite films and the corresponding drug-loaded films, these two crystalline peaks still exist, but the intensities are weaker. It is evident that the addition of OREC greatly changed the crystallinity of chitosan, again confirming the strong interaction between chitosan and OREC. In addition, it is most likely that amino and hydroxyl groups in chitosan hydrogen bond with BSA, which then resulted in an amorphous structure of the polymer complex (Anh, Choi, & Cho, 2001).

In the SEM images of the upper surfaces and the fracture surfaces of chitosan *per se* and chitosan/OREC nanocomposite films and corresponding drug-loaded films (Fig. 3), the upper surface of the film of chitosan itself on its own is very smooth, whilst the surfaces of the nanocomposite films are significantly different, obviously due to the

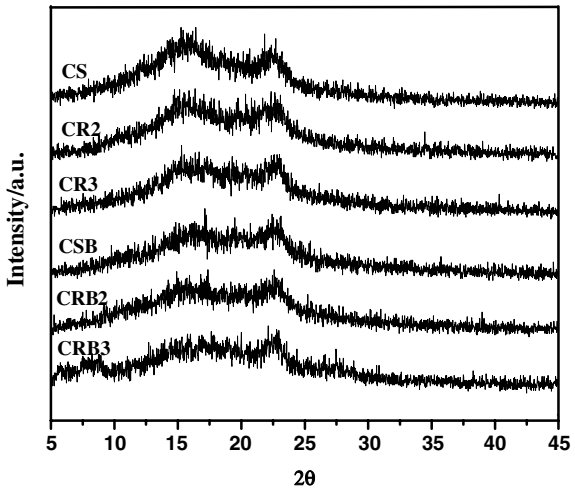

Fig. 2. XRD patterns of chitosan and the nanocompopsite films and their drug-loaded films.

presence of the rectorite particles which are distributed uniformly on the upper surface of all the nanocomposite films.

Furthermore, the fracture surface of chitosan is also smooth, even CR4 with 5 wt% OREC has a smooth fracture surface, while as the amount of OREC increases, the fracture surfaces of the nanocomposite films become rougher. These surface differences can be expected to greatly influence the mechanical properties of the materials. It was also found that the incorporation of model drugs into the films resulted in a significant change of fracture morphologies. Their cross sections are rough and some deficiencies are observed. These results further suggest that the introduction of OREC and BSA changed the crystallinity of pure chitosan film (Wang et al., 2005), which are in good agreement with the XRD analysis.

3.2. Characteristic study

As shown in Table 1, in comparison with pure chitosan film, the water vapor permeability (WVP) of the chitosan/OREC nanocomposite films decrease in an obvious manner, and the minimum of 2.28×10^{-8} g mm mm^{-2} h^{-1} mm^{-1}Hg is achieved when the interlayer distance of the layered silicate is the largest (CR3). It is quite clear that water barrier capacity of the chitosan/OREC nanocomposite films is improved. The results may be related to the silicate layers with a large aspect ratio (length of rectorite layer about 100–200 nm, thickness of a rectorite layer about 2 nm) dispersing into the chitosan matrix. When small liquid molecules attempt to permeate into the multiple layer matrixes, they must go around the silicate layers; this effectively lengthens the molecular permeation route (Kim, Hu, Woo, & Sham, 2005). The effect is that the water is not so easily able to get through the nanocomposite films in comparison with the case of pure chitosan film (Fig. 4). Moreover, it was found that the WVP value decreases further as the effective routes are increased with improvements

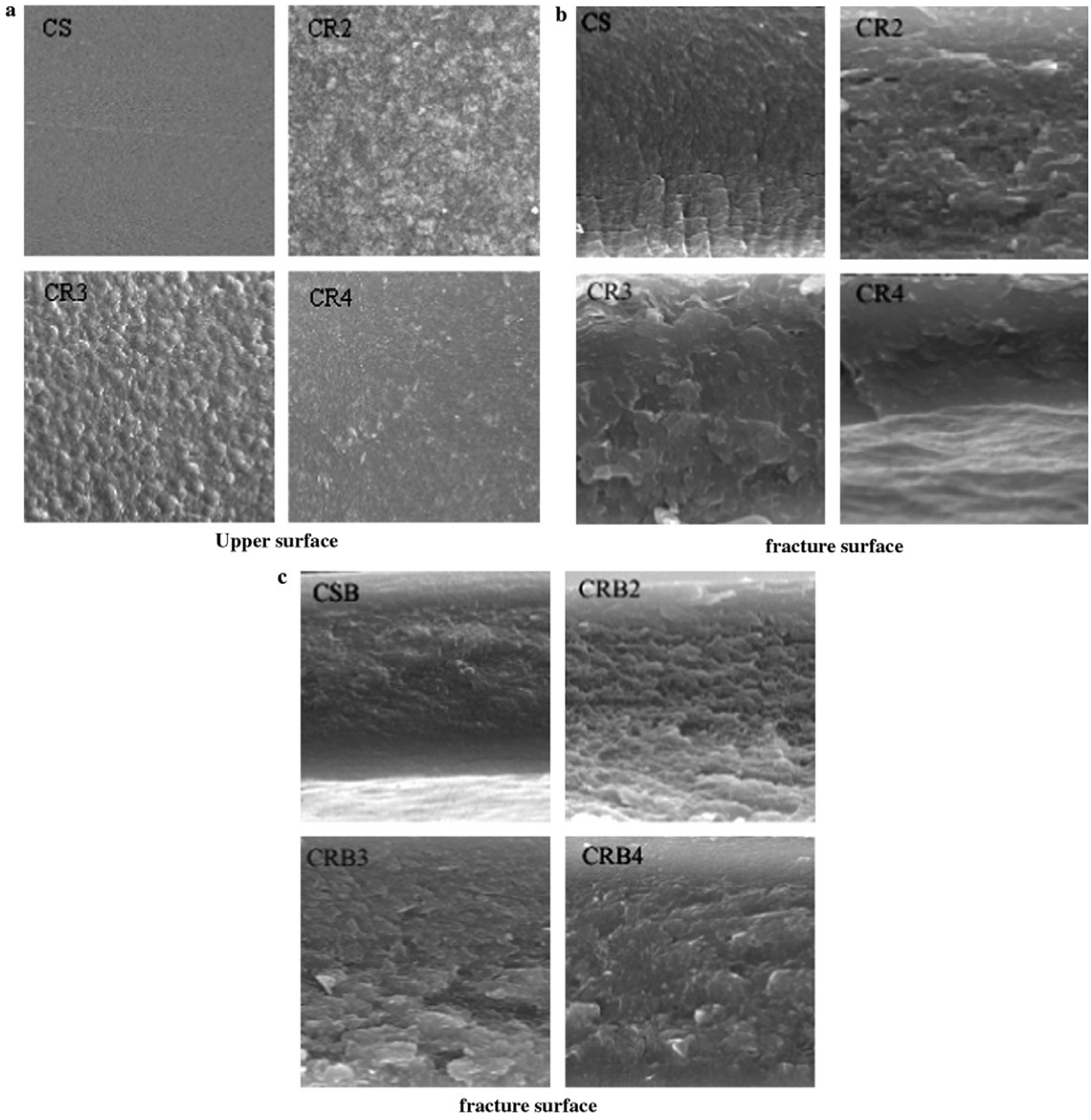

Fig. 3. SEM micrographs of chitosan and CS/OREC nanocomposite films. (a) Upper surface and (b,c) fracture surface.

Table 1
Water barrier and mechanical properties and optical transmittance of chitosan and CS/OREC nanocomposite films

Samples	WVP ($\times 10^{-8}$ g mm mm^{-2} h^{-1} mm^{-1}Hg)	Q (%)	σ_b (MPa)		ε_b (%)		(T) (%)
			Dry	Wet	Dry	Wet	
CS	4.84	60.02	55.61	22.56	11	35	90
CR1	3.10	10.60	12.53	10.10	3	20	65
CR2	3.26	18.23	24.86	13.42	5	31	75
CR3	2.28	15.30	38.95	22.09	9	35	80
CR4	3.67	27.45	56.58	23.93	12	39	83
CR5	4.38	45.25	59.71	25.92	14	45	87

in the dispersion of OREC in chitosan system (Liu, Hoa, & Pugh, 2005). In this system, CR3 has the largest interlayer distance and thereby involved the best dispersion of clay; accordingly CR3 show the lowest value of WVP. In general, the higher the proportion of OREC in the nanocomposites, the lower the value of WVP.

Similarly, due to water barrier effects, that is the impermeable clay platelets making the pathway for water to

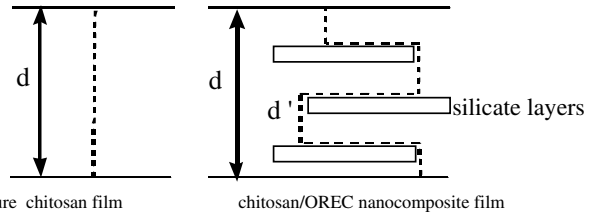

Fig. 4. The simple barrier model of polymer/layered silicate nanocomposites.

enter the nanocomposite films tortuous (Becker, Varley, & Simon, 2004; Liu et al., 2005), the nanocomposite films have low values of water uptake, as evidenced in Table 1. The number of the silicate layers is higher and the interlayer distance is larger, which make it harder for water to be absorbed into the film. Therefore, CR1 with the highest amount of OREC and CR3 with the largest interlay distance show the least water content.

The tensile strength (σ_b) and the elongation at break (ε_b) of the nanocomposite films in the dry state increase with the decrease of the amount of OREC (Table 1), and in comparison with pure chitosan film, the mechanical property is improved only when the mass ratio of chitosan to OREC is 20:1 (CR4) and 50:1 (CR5). The reason for this could be that the distribution in nano-size of a few OREC particles in the chitosan matrix acted as the part cross-linked sections (Chen, Tien, & Wei, 1999), resulting in the increase of the mechanical property. However, the high amount of OREC may cause the collapse of the mechanical stabilities/properties of polymer/layered silicate nanocomposites (Ma, Lu, Liang, & Yan, 2004; Phang et al., 2005), a fact corroborated by the SEM images (Fig. 3). Here, the fracture surface is nearly smooth and no microvoids are seen when the amount of OREC is low, while rough supper surface, rough fracture surface, and even some microvoids are seen when the amount of OREC is more than 5 wt%. Interestingly, with the help of the water barrier activity of the layered silicate, the mechanical properties of the nanocomposite films in the wet state increased rapidly corresponding to chitosan film when the mass ratio of chitosan to OREC was more than 12:1. It is therefore obvious that chitosan/OREC nanocomposite films are more suitable for application to food packaging industry in the wet state than chitosan film.

Pure chitosan film is transparent; the optical transmittance at a wavelength of 800 nm is 90% (Table 1). Optical clarity of all the nanocomposite films was well-retained in high transparency because of the nanoscale dispersion of the silicates in the chitosan matrix (Strawhecker & Manias, 2000), but with the increase of the amount of OREC, the optical transmittance of the nanocomposite films decreased gradually (Table 1). This phenomenon can be attributed to the aggregation trend of clay particles with increasing OREC content (Koo, Ham, Choi, Kim, & Chung, 2003; Wang et al., 2005) as proved by the SEM analysis of the upper surface of the films in Fig. 3a.

Table 2
Ultraviolet-screen rate of chitosan and CS/OREC nanocomposite films

Wavelength (nm)	CS	CR1	CR2	CR3	CR4	CR5
297	60.60	92.96	89.54	95.41	76.08	74.13
313	57.80	91.43	89.23	95.04	74.26	72.17
350	41.10	85.10	84.24	88.90	64.71	62.08
366	35.91	82.50	81.24	85.00	61.00	57.76
400	29.00	77.89	76.57	79.37	56.12	52.12
Mean	44.88	85.98	84.16	88.74	66.43	63.65

The ultraviolet-screen rates, determined by measuring the transmission of the UV light of chitosan and the nanocomposites films, (Table 2) clearly demonstrate that CR3 shows the highest screen rate of UV light, which is consistent with the intercalation effect with the largest interlayer distance. The screen rate of UV light of CR1 is higher than that of CR5 although their Δd_L values are equivalent; this reveals that the anti-ultraviolet capacity is also related to the amount of OREC; with the increase of OREC, the anti-ultraviolet capacity is improved. The same result can be also observed from CR2 and CR4 (Table 2). Therefore, conclusions can be drawn that the chitosan/OREC nanocomposites have excellent anti-ultraviolet activity, which is directly proportional to both the Δd_L value and the content of OREC. This is not surprising as the typical silicate layer lateral sizes are 50–1000 nm (Strawhecker & Manias, 2000). The large value for the refractive index of calcium rectorite is helpful in conferring ability to screen strongly against ultraviolet rays; calcium rectorite can scatter forcefully the UV rays due to its very small particle size (Wang & Guo, 2004).

3.3. Bactericidal activity

The inhibitory effects of pure chitosan film and the chitosan/REC nanocomposite films on *S. aureus* and *E. coli* growths (Table 3) all show better bactericidal activity nanocomposite films as compared to pure chitosan film.

The exact mechanism of the antimicrobial activity of chitosan is still unknown. But it has been generally accepted that the all-important factor is the positive charge on the C-2 of the glucosamine monomer at below pH 6.3

Table 3
Bactericidal effects of chitosan film and CS/OREC nanocomposite films against microorganisms

Samples	*Staphylococcus aureus*		*Escherichia coli*	
	No. of colonies	Killing rate (%)	No. of colonies	Killing rate (%)
Control	2.7×10^6	–	2.3×10^6	–
Chitosan	6.4×10^5	77.7	6.8×10^5	70.4
CR1	3.0×10^3	99.9	2.1×10^5	90.8
CR2	8.2×10^4	97	4.5×10^5	80.4
CR3	4.3×10^3	99.9	2.8×10^5	87.8
CR4	1.3×10^5	95.2	4.9×10^5	78.7
CR5	2.8×10^5	89.6	5.1×10^5	77.8

(Helander, Nurmiaho-Lassila, Ahvenainen, Rhoades, & Roller, 2001; Papineau, Hoover, Knorr, & Farkas, 1991). $-NH_3^+$ in chitosan solution could interact vigorously with phosphoryl groups of phospholipids in cell membranes, so damaging the membranes (Liu, Du, Wang, Hu, & Kennedy, 2004). On the other hand, it was reported that the layered rectorite silicate could surfacely absorb the bacteria from the solution and immobilize the bacteria (Lemke et al., 2001), on account of the significant adsorption capacities of such layered materials.

In this study system, the antibacterial process of chitosan/OREC nanocomposites may be divided into two stages. The first stage is the adsorption of the bacteria from solution and immobilization on the surface of the clay. The second stage is related to the accumulation of chitosan on the surface of clay. Chitosan around the layered silicate may have more chance to inhibit the growth of bacteria; besides, chitosan chains are in order and aggregate when confined in the interlayer of the silicate, so that positive charge (amino group) density in each unit volume is increased by the chitosan chains aggregating between the rectorite interlayers, i.e. positive charge (amino group) density in *each unit volume* is increased. Hence, the nanocomposite films have better inhibitory effect on the growth of bacteria. Another possible reason for enhanced antibacterial activity may be a cooperative effect between chitosan, rectorite, and CTAB, but this needs to be investigated and proved.

In addition, it is clearly found that CR1 film with the highest amount of OREC and CR3 film with the largest interlayer distance exhibit the strongest antibacterial behavior (Table 3). As the amount of OREC increases, the effective layers in unit weight may increase because of good dispersion (see SEM results Fig. 3), thereupon larger specific surface areas are obtained, and more bacteria are adsorbed and immobilized onto the surface of the clay, then chitosan inhibits them. In the same way, with the increase of the interlayer distance, specific surface areas of the layers also become greater; also more chitosan chains are inserted into the interlayer and positive charge density in each unit volume further increase. In this way, chitosan may have more chance to inhibit the growth of bacteria. Therefore, alternatively, the increase of the amount or the interlayer distance may result in the improvement of the inhibitory activity against Gram-positive bacteria.

3.4. In vitro release studies

The BSA *in vitro* release behavior of chitosan and chitosan/OREC nanocomposite films containing BSA (Fig. 5) show similar release profiles, and exhibit a small burst release in the first 12 h and then slow constant release but with different rates. Interestingly, all films show equivalent drug release in the initial stages. But after several hours, all nanocomposite films show slower release in comparison to pure chitosan film.

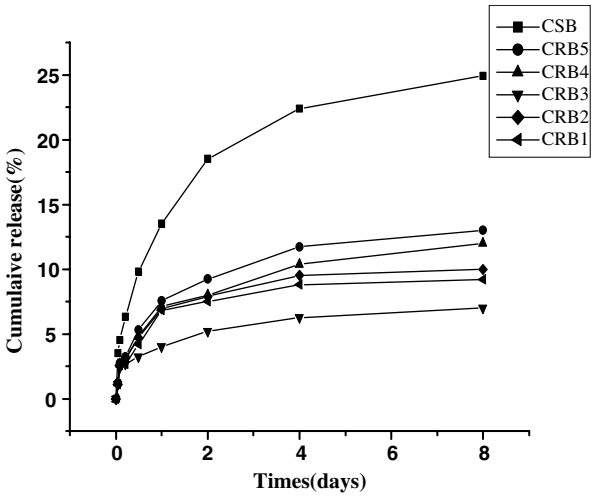

Fig. 5. *In vitro* release profiles of BSA from the chitosan/OREC nanocomposite films.

This initial burst effect could be attributed to the diffusion of the drug caused by rapid membrane swelling and also the faster release of the drug adsorbed toward the surface of the films matrix (Wang & Hon, 2005). So at the beginning, all films have similar swelling behavior and the equivalent rates of release of drug. This is particularly noticeable since a macromolecular model was used.

It is worthwhile to note that the nanocomposite films, especially CRB3 with the largest interlayer distance, exhibit the subsequent slowest sustained release, and with the increase of the amount of OREC, the releases are slower. It is generally accepted that increased hydrophobicity and electrostatic attractive forces could improve the controlled-drug release properties (Liu, Li, Zhao, Yao, & Liu, 2002; Perugini et al., 2003). Another literature reported that the release of drug was controlled by the swelling behavior of the materials (Rujiravanit et al., 2003). In this system, firstly, as shown by FTIR-ATR analysis, electrostatic interaction between chitosan, OREC, and BSA surely occurred. Furthermore, just like the analysis of the water vapor permeability (WVP) which was measured according to an ASTM method and the water uptake (Q%) which was assessed according to ISO62-1980 (E) as described in Section 3.2, the value of WVP and the water content of the nanocomposite films are just related to the relative amounts and the interlayer distances of OREC, CR1 with the highest amount of OREC (sample code CR1) and CR3 with the largest interlay distance show much lower value of WVP and much less water content than does chitosan film. In other words, CR1 and CR3 exhibit much better hydrophobicity than does chitosan film. In addition, the literature (Cypes, Saltzman, & Giannelis, 2003) reported that this reduction of the drug-release rate for polymer/layered silicate nanocomposites was a function of volume fraction of silicate in the composite, as well as the aspect ratio of the silicate layers. So from the above analysis, it is certain that the chitosan/OREC nanocomposite films have excellent drug-controlled release properties. Furthermore, clay can

provide mucoadhesive and toxin adsorption capabilities, which further suggest strongly that chitosan/OREC nanocomposite films are quite suitable to be applied in drug-delivery systems in comparison with pure chitosan film.

4. Conclusions

The addition of OREC to pure chitosan film influenced many of the properties. These properties enhancements were related to the amount and the interlayer distance of the layered silicate in the chitosan/OREC nanocomposite films. Therefore, it can be predicted that a combination of the appropriate amount and interlayer distance can be optimized in a single device in order to achieve any desired combination of material properties. This characteristic of the layered silicate additives is potentially important in the formulation of polymer composites for antimicrobial food packaging antimicrobial agent, water-barrier compound and anti-ultraviolet compound and for drug-delivery systems as drug-controlled release carrier.

Acknowledgment

We are grateful for the financial support of this research from National Science Foundation of China (Grant No. 29977014).

References

Anh, J. S., Choi, H. K., & Cho, C. S. (2001). A novel mucoadhesive polymer prepared by template polymerization of acrylic acid in the presence of chitosan. *Biomaterials, 22*, 923–928.

Avella, M., De Vlieger, J. J., Errico, M. E., Fischer, S., Vacca, P., & Volpe, M. G. (2005). Biodegradable starch/clay nanocomposite films for food packaging applications. *Food Chemistry, 93*, 467–474.

Becker, O., Varley, R. J., & Simon, G. P. (2004). Thermal stability and water uptake of high performance epoxy layered silicate nanocomposites. *European Polymer Journal, 40*, 187–195.

Carretero, M. I. (2002). Clay minerals and their beneficial effects upon human health. *Applied Clay Science, 21*, 155–163.

Chen, T. K., Tien, Y. I., & Wei, K. H. (1999). Synthesis and characterization of novel segmented polyurethane clay nanocomposite via poly-(epsilon-caprolactone)/clay. *Journal of Polymer Science: Part A-Polymer Chemistry, 37*, 2225–2233.

Cypes, S. H., Saltzman, W. M., & Giannelis, E. P. (2003). Organosilicate-polymer drug delivery systems: controlled release and enhanced mechanical properties. *Journal of Controlled Release, 90*, 163–169.

Darder, M., Colilla, M., & Hitzky, E. R. (2003). Biopolymer-clay nanocomposites based on chitosan intercalated in Montmorillonite. *Chemistry of Materials, 15*, 3774–3780.

Dong, Y. C., & Feng, S. S. (2005). Poly (D,L-lactide-co-glycolide)/montmorillonite nanoparticles for oral delivery of anticancer drugs. *Biomaterials, 26*, 6068–6076.

Helander, I. M., Nurmiaho-Lassila, E. L., Ahvenainen, R., Rhoades, J., & Roller, S. (2001). Chitosan disrupts the barrier properties of the outer membrane of Gram-negative bacteria. *International Journal of Food Microbiology, 71*, 235–244.

Iborra, C. V., Cultrone, G., Cerezo, P., Aguzzi, C., Baschini, M. T., VallÃÃs, J., et al. (2006). Characterisation of northern Patagonian bentonites for pharmaceutical uses. *Applied Clay Science, 31*, 272–281.

Kim, J. K., Hu, C., Woo, R. S. C., & Sham, M. L. (2005). Moisture barrier characteristics of organoclay–epoxy nanocomposites. *Composites Science and Technology, 65*, 805–813.

Koo, C. M., Ham, H. T., Choi, M. H., Kim, S. O., & Chung, I. J. (2003). Characteristics of polyvinylpyrrolidone-layered silicate nanocomposites prepared by attrition ball milling. *Polymer, 44*, 681–689.

Lemke, S. L., Ottinger, S. E., Mayura, K., Ake, C. L., Pimpukdee, K., Wang, N., et al. (2001). Development of a multi-tiered approach to the in vitro prescreening of clay-based enterosorbents. *Animal Feed Science and Technology, 93*, 17–29.

Li, Z., Du, Y. M., Zhang, L. N., & Pang, D. W. (2003). Preparation and characterization of CdS quantum dots chitosan biocomposite. *Reactive and Functional Polymers, 55*, 35–43.

Liu, H., Du, Y. M., Wang, X. H., Hu, Y., & Kennedy, J. F. (2004). Interaction between chitosan and alkyl b-D-glucopyranoside and its effect on their antimicrobial activity. *Carbohydrate Polymers, 56*, 243–250.

Liu, W. P., Hoa, S. V., & Pugh, M. (2005). Fracture toughness and water uptake of high-performance epoxy/nanoclay nanocomposites. *Composites Science and Technology, 65*, 2364–2373.

Liu, W. G., Li, F., Zhao, X. D., Yao, K. D., & Liu, Q. G. (2002). Atom force microscopic characterisation of the interaction forces between bovine serum albumin and cross-linked alkylated chitosan membranes in media of different pH. *Polymer International, 51*, 1459–1463.

Lopez, C. R., & Bodmeier, R. (1997). Mechanical, water uptake and permeability properties of crosslinked chitosan glutamate and alginate films. *Journal of Controlled Release, 44*, 215–225.

Ma, X. Y., Lu, H. J., Liang, G. Z., & Yan, H. X. (2004). Rectorite/thermoplastic polyurethane nanocomposites: preparation, characterization, and properties. *Journal of Applied Polymer Science, 93*, 608–614.

Papineau, A. M., Hoover, D. G., Knorr, D., & Farkas, D. J. (1991). Antimicrobial effect of water-soluble chitosans with high hydrostatic pressure. *Food Biotechnology, 5*, 45–57.

Perugini, P., Genta, I., Conti, B., Modena, T., & Pavanetto, F. (2003). Periodontal delivery of ipriflavone: new chitosan/PLGA film delivery system for a lipophilic drug. *International Journal of Pharmaceutics, 252*, 1–9.

Petersen, K., Nielsen, P. V., Bertelsen, G., Lawther, M., Olsen, M. B., Nilsson, N. H., et al. (1999). Potential of biobased materials for food packaging. *Trends in Food Science & Technology, 2*, 52–68.

Phang, I. Y., Liu, T. X., Mohamed, A., Pramoda, K. P., Chen, L., Shen, L., et al. (2005). Morphology, thermal and mechanical properties of nylon 12/organoclay nanocomposites prepared by melt compounding. *Polymer International, 54*, 456–464.

Phillips, T. D., Lemke, S. L., & Grant, P. G. (2002). Characterization of clay-based enterosorbents for the prevention of aflatoxicosis. *Advances in Experimental Medicine and Biology, 504*, 157–171.

Qin, C. Q., Du, Y. M., & Xiao, L. (2002). Effect of hydrogen peroxide treatment on the molecular weight and structure of chitosan. *Polymer Degradation and Stability, 76*(2), 211–218.

Ravi, K., & Majeti, N. V. (2000). A review of chitin and chitosan applications. *Reactive and Functional Polymers, 1*, 1–27.

Rujiravanit, R., Kruaykitanon, S., Jamieson, A. M., & Tokura, S. (2003). Preparation of crosslinked chitosan/silk fibroin blend films for drug delivery system. *Macromolecule Bioscience, 3*, 604–611.

Shahidi, F., Arachchi, J. K. V., & Jeon, Y. J. (1999). Food applications of chitin and chitosans. *Trends in Food Science & Technology, 10*, 37–51.

Strawhecker, K. E., & Manias, E. (2000). Structure and properties of poly (vinyl alcohol)/Na^+–Montmorillonite nanocomposites. *Chemistry Materials, 12*, 2943–2949.

Vilivalam, V. D., & Dodane, V. (1998). Pharmaceutical applications of chitosan. *Pharmaceutical Science & Technology Today, 6*, 246–253.

Wang, J. W., & Hon, M. H. (2005). Preparation of poly(ethylene-glycol)/chitosan membranes by a glucose-mediating process and in vitro drug release. *Journal of Applied Polymer Science, 96*, 1083–1094.

Wang, L. Y., & Guo, J. (2004). Rheological and antiultraviolet properties of polypropylene/ montmorillonite nanocomposites. *Journal of Dalian Institute of Light Industry, 2*, 136–139.

Wang, Q., Du, Y. M., & Fan, L. H. (2005). Properties of chitosan/ poly(vinyl alcohol) films for drug-controlled release. *Journal of Applied Polymer Science, 96*, 808–813.

Wang, X. Y., Du, Y. M., Yang, J. H., Wang, X. H., Shi, X. W., & Hu, Y. (2006). Preparation, characterization and antimicrobial activity of chitosan/layered silicate nanocomposites. *Polymer, 47*, 6738–6744.

Wei, Y. C., Hudson, S. M., & Mayer, J. M. (1992). The crosslinking of chitosan fibers. *Journal of Polymer Science Part A: Polymer Chemistry, 30*, 2187–2193.

Xu, J., McCarthy, S. P., & Gross, R. A. (1996). Chitosan film acylation and effects on biodegradability. *Macromolecules, 29*, 3436–3440.

Zhao, L. Q., Wang, C. X., & Hu, Z. F. (2004). Reasearch for rectorite as natural cosmetics and health-care materials. *Chinese Journal of Non-metal Industry, 6*, 18–22.